Photoproduction of Charged π Mesons from Nuclei*

W. MELVILLE MCCLELLAND†
Laboratory of Nuclear Studies, Cornell University, Ithaca, New York
(Received March 6, 1961)

The photoproduction of charged π mesons by a 1000-Mev bremsstrahlung beam has been studied for the elements Be, C, Al, Cu, and Pb. Mesons with energies in the range 100 to 400 Mev emerging from the targets at angles of 58° and 115° were detected, and absolute measurements for the cross section are given. An optical model for the nucleus was employed to predict absolute upper and lower limits for the nuclear cross section, and reasonable agreement with the data was obtained. The measured cross sections had a dependence on the target atomic weight of $A^{\frac{3}{4}}$ and this result lay between the limits predicted by the model. The experimental nuclear π^-/π^+ ratio exhibited the general behavior of this quantity for deuterium, but the model could make no prediction here. The results seem to be consistent with an optical model treatment of an assumed initial production of mesons throughout the nuclear volume, and no recourse to a surface production mechanism was found to be necessary.

I. INTRODUCTION

THE photoproduction of π mesons from complex nuclei can be used to investigate the interaction of these mesons in nuclear matter. Previous studies[1–8] have indicated that the meson yield varies with the atomic weight of the target nuclei approximately as $A^{\frac{3}{4}}$. This result seems to hold true for both charged and neutral mesons with energies from essentially zero to 150 Mev and for a wide range of target materials.

Two models have been proposed to explain this observed behavior of the yield. The first employs the impulse approximation[9–12] and assumes that the production of mesons occurs throughout the nuclear volume. The escape of the mesons from the nucleus can then be calculated using an optical model and the dependence of the yield on the target atomic weight obtained in this way agrees with the observed results. The second suggestion[13,14] assumes that some mechanism actually suppresses photoproduction on interior nucleons, leaving only the surface nucleons to serve as targets. The yield would thus depend on the relative number of nucleons comprising the nuclear surface. Actually the success of the optical-model approach to the volume-production scheme relies on the fact that the meson interaction mean free path in nuclear matter is smaller than the nuclear size. For all but very low meson energies this seems to be the case and the model has been applied with varying degrees of success by many authors.

The present experiment was undertaken with the object of extending such measurements to mesons of still higher energy. Absolute values of the nuclear cross section were obtained for several meson energies and target materials. In addition, the dependence of the cross section on the atomic weight was determined to be approximately $A^{\frac{3}{4}}$. Furthermore, when the relative numbers of neutrons and protons were taken into account, the ratio of the negative to positive meson yields was found to vary essentially as does the same quantity for deuterium. The experimental results will be presented first and these will be followed by a possible interpretation based on the ideas of the volume-production model. It will be found that no recourse to a surface-production mechanism is necessary, and if such a process does occur, its effect is indistinguishable from the uncertainties in the volume-production model which was employed.

II. EQUIPMENT AND PROCEDURE

The Cornell 1.2-Bev electron synchrotron was used to accelerate electrons to a peak energy of 1000 Mev and this beam was allowed to strike an internal tungsten target. The resulting bremsstrahlung beam passed through the wall of the donut and on through a lead collimator. This collimated gamma-ray beam was passed through the gap of a permanent magnet to sweep out charged particles and was then monitored by a thin ionization chamber located on the downstream side of a lead-lined channel in the main concrete wall used to shield the experimental area from the background radiation of the machine. The various targets were placed

* Supported by the joint program of the Office of Naval Research and the U. S. Atomic Energy Commission.

† Present address: Lawrence Radiation Laboratory, University of California, Livermore, California. This paper is based on a thesis submitted to the Graduate School of Cornell University in partial fulfillment of the requirements for the degree of Doctor of Philosophy.

[1] R. F. Mozley, Phys. Rev. **80**, 493 (1950).
[2] W. K. H. Panofsky, J. N. Steinberger, and J. Stetler, Phys. Rev. **86**, 180 (1952).
[3] R. M. Littauer and D. Walker, Phys. Rev. **86**, 838 (1952).
[4] W. S. C. Williams, K. M. Crowe, and R. M. Friedman, Phys. Rev. **105**, 1840 (1957).
[5] J. R. Waters, Phys. Rev. **113**, 1133 (1959).
[6] W. Imhof, E. A. Knapp, H. Easterday, and V. Perez-Mendez, Phys. Rev. **108**, 1040 (1957).
[7] A. S. Belousov, V. M. Popova, N. G. Semashko, E. V. Shitov, E. I. Tamm, V. I. Veksler, and F. R. Iagudina, *Proceedings of the CERN Symposium on High-Energy Accelerators and Pion Physics, Geneva, 1956* (European Organization of Nuclear Research, Geneva, 1956), Vol. II, p. 288.
[8] A. S. Belousov, S. V. Rusakov, and E. I. Tamm, Soviet Phys.—JETP **8**, 247 (1959).
[9] K. A. Brueckner, R. Serber, and K. M. Watson, Phys. Rev. **84**, 258 (1951).
[10] N. C. Francis and K. M. Watson, Am. J. Phys. **21**, 659 (1953).
[11] K. W. McVoy, Ph.D. thesis, Cornell University, 1956 (unpublished).
[12] A. S. Belousov, B. B. Govorkov, and V. I. Gol'danskii, Soviet Phys.—JETP **9**, 164 (1959).
[13] S. T. Butler, Phys. Rev. **87**, 1117 (1952).
[14] R. R. Wilson, Phys. Rev. **86**, 125 (1952); **104**, 218 (1956).

in this monitored beam and a strong-focusing magnet was used to focus the emergent charged particles on a counter telescope. The spectrometer thus selected particles having the desired charge, momentum, and direction upon leaving the target material. All of the electronic equipment associated with the telescope was located in another room, where the information from the counters was recorded.

The peak energy of the bremsstrahlung beam is determined by the energy of the electrons at the time of their impact with the tungsten target. The actual time of impact, and hence the energy of the electrons, was determined by shaping the rf cavity voltage. In practice, the cavity voltage is programed to result in a spread of electron energies incident on the tungsten target. Throughout the experiment the mean electron energy was kept at 1000 Mev with a beam spread of about 1 msec or ± 20 Mev at most. The energy of the electrons at impact was measured by integrating the magnet voltage from injection time to the time of impact, the integral being proportional to the magnetic field at this particular time. This system was calibrated against actual magnetic field measurements made with a rotating-coil probe and a further calibration was carried out by measuring the end point of the bremsstrahlung spectrum with a pair spectrometer.

The standard beam monitor at this laboratory is an ionization chamber designed by Wilson.[15] The charge collected on the plates is proportional to the total energy in the incident photon beam and this proportionality constant has been calculated and experimentally verified to $\pm 5\%$. The output current from the quantameter is integrated electronically[16] and the local unit of absorbed beam is called a "sweep." It is convenient to give counting rates in the units of "counts per sweep."

Actually, for this experiment the quantameter described above was not used as the primary beam monitor. Being essentially a total absorption chamber, it must be located downstream from the experimental area. But in the present work various target materials were introduced to the photon beam and hence the monitoring would depend upon the particular target used. To avoid this situation a thin ionization chamber was located ahead of the experimental target position and frequent calibration against the quantameter was carried out. With this scheme a collimated monitored gamma-ray beam could be directed on any target independent of the target material or length.

The magnet used in this experiment to focus charged particles on the counter telescope was of the strong-focusing variety. The two-lens arrangement, a positive lens followed by a negative one, bent particles through an angle of 35°. The n value was ± 30 and the average radius of curvature was 200 cm. This system resulted in a vertical magnification of approximately 5 and a corresponding radial one of $\frac{1}{5}$.

[15] R. R. Wilson, Nuclear Instr. **1**, 101 (1957).
[16] R. M. Littauer, Rev. Sci. Instr. **25**, 148 (1954).

The excitation of the magnet is measured with a standard shunt and potentiometer. The calibration curve for the magnet was determined by measuring a series of range curves for protons using copper absorbers and the usual counter telescope. Saturation effects become noticeable above a momentum of 500 Mev/c. A confirmation of the calibration from the range curves was obtained from measurements made using the technique of a current-carrying wire. Rotating coil measurements showed that for momenta below 550 Mev/c a value of 30 for n is a good approximation over most of the magnet channel width. The solid angle subtended by the detection system at the target was measured by calibration against another counter telescope of calculable solid angle. Measurements of the counting rate from a thin target as a function of its position along the beam line indicate that the aperture of the magnet is quite uniform over a target length of 3 in. or more. This is in agreement with orbit calculations and it indicates the consequences of the radial magnification value given above.

The basic counter system associated with the detection magnet consisted of four scintillation counters arranged to form two three-counter telescopes. This arrangement was used for the measurements made at 115°, but modifications were necessary at 58°. Each counter consisted of a sensitive detecting material connected optically to a photomultiplier tube by means of a Lucite light pipe. NE 102 plastic scintillator made by Nuclear Enterprises Ltd. was used for the detector and the tubes were RCA 6342's. Each counter was $\frac{1}{4}$ in. thick, resulting in a resolution of 40%. Counters No. 3 and 4 were 3 in. high and 2 cm wide; they were located at the focal point of the magnet and served to define two adjacent momentum channels. Counter No. 1 placed ahead of these and counter No. 2 the same distance behind completed the dual three-counter telescope system, 1–3–2 and 1–4–2. Each phototube was wrapped in magnetic shielding and mounted in a box of magnet iron attached to a horizontal platform rigidly fixed to the magnet.

Because of the possible presence of electrons at 58° the telescope was altered in several respects. Most important of these was the addition of a 6-in. diameter, 9-in. long lead-glass Čerenkov counter placed behind the telescope with a different No. 2 counter used as a defining counter for it. The index of refraction of the lead glass was 1.65 with a radiation length of 2.8 cm.

Standard counting techniques were used, although the arrangements were somewhat different for the two angles. Amplified pulses were fed to two discriminator circuits, D and D', which had variable biases. The shaped output pulses were used in coincidence circuits which had a resolving time of about 0.3 μsec. In general, biases in D were set low to count minimum ionizing particles and those in D' high to miss them. Because of general background radiation in the synchrotron room the discriminators were gated on toward the end of each cycle for an interval of 2 msec, which covered the dura-

tion of the photon beam. The singles rate of each counter was recorded on a separate scaler and in addition six other scalers recorded various coincidence outputs. Any pulse large enough to get through D' would veto the final output. A 28-channel pulse-height analyzer was used to monitor some counter during each run. All biases were set on the basis of such pulse-height distributions, the analyzer being triggered by any of the six coincidence outputs. Counting rates were sufficiently low so that accidental coincidences were negligible.

By several means it was established that electrons constituted at most a neglibigle fraction of the total counts detected at 115°. At 58°, however, there was evidence of electron contamination in the meson yields, so the telescope was modified. The two angles will thus be treated separately here.

At 115° it was necessary to discriminate against only protons. Copper absorbers placed between counters in the telescope stopped protons for the lower momentum runs. At higher energies enough absorber was added to stop most of the protons and to retard appreciably any which did not stop. The D biases for all four counters were set just low enough to pass all minimum ionizing particles as well as slower ones. Threefold coincidences of such pulses could be due to either a meson or a proton. To distinguish between the two the D' discriminator utilized the fact that protons having the same momentum as the mesons will yield a much larger pulse, particularly in counter No. 2 located after the copper absorber. In addition, it was helpful to reject immediately any particle which made a large pulse in counter No. 1. The veto scheme thus operated by using counters No. 1 and 2 with the D' biases; a large pulse in either counter or in both would reject the threefold coincidence. Any coincidence not vetoed should be due to the passage of a meson through the telescope.

Because one object of this experiment was to measure the π^-/π^+ ratio, it was essential that no property of the detection system change upon reversal of the magnet polarity. To this end the pulse-height distribution in each counter was recorded using carbon as a target for each meson momentum studied, and for both the π^- and π^+ runs. A comparison of these pulse-height distributions served as a check on the effectiveness of the proton rejection scheme.

At 58° both electrons and protons had to be rejected. The protons were dealt with as before, but the electrons proved difficult to distinguish from the mesons of the same momentum. While the protons contaminated only π^+ runs, so that π^- runs could be used to check the rejection scheme, no such advantage existed for electrons and positrons.

The Čerenkov counter was not included in the main telescope; it was used solely as an electron veto counter on the two threefold coincidences. The relative number of electrons present at 58° was reasonably small, even from the lead target, so the lead-glass counter could be used to reject these with some confidence. A high bias was used to ignore all mesons and any resulting pulses were considered to be electrons, which then vetoed the coincidence. Actually, μ mesons from π decays in flight would probably make large pulses also, but the correction for this was negligible. Also the effect of the electrons from π-μ-e decays in the lead glass was of no importance because of the time delay. The electrons could also shower in the copper absorbers between counters and thus give a pulse greater than minimum ionizing. Any large pulse, then, in No. 1, 2, 3, or 4 was undesirable, whether it be a proton or an electron, and all four were used as veto counters. Any threefold coincidence (which required that each pulse be above its D bias) which was not vetoed by a characteristically large proton or electron pulse was considered to be a π meson.

The target materials studied in this work were Be, C, Al, Cu, and Pb. The beryllium target was a cylinder 2 in. in diameter and the other four targets were 3 in. square. Each of the latter four targets was about 0.3 radiation length long while the beryllium was 0.1 radiation length. All of the targets were placed normal to the gamma-ray beam.

III. EVALUATION OF THE CROSS SECTION

First a general expression for the photoproduction cross section of π mesons from a nuclear target will be given. The case of a hydrogen target is a particular example of this expression. The measured counting rates of mesons must be corrected for various experimental effects before they can be used in such an expression for the cross section. The corrections will be discussed here and the results will be presented in Sec. IV.

A. Expression for the Cross Section

Let N equal the number of mesons per sweep produced in a target of atomic weight A by a bremsstrahlung beam of peak energy k_0 and having momenta between p and $p+\Delta p$ and directions between Ω and $\Omega+\Delta\Omega$. Then N is given by an expression of the form

$$N=\int\int d\Omega dT\,\alpha(\theta,\varphi,p)\int n\frac{d^2\sigma(T,\Omega,k)}{dTd\Omega}n(k)dk.$$

Here n is the number of target nuclei per cm^2, $n(k)$ is the bremsstrahlung distribution function, T is the kinetic energy of the meson, and $\alpha(\theta,\varphi,p)$ defines the $\Delta\Omega$ and Δp accepted by the detector. Furthermore, a quantity Q, the number of equivalent quanta per sweep, may be defined by the relation

$$k_0Q\equiv\int_0^{k_0}kn(k)dk,$$

where k_0 is the maximum energy of the bremsstrahlung beam. $kn(k)$ is practically constant, however, and may be written as $kn(k)=Qf(k)$, where $f(k)$ simply gives

the deviation of $kn(k)$ from a constant value. Then one obtains

$$\frac{N}{nQmp(dT/dp)}=\int_0^{k_0}\frac{d^2\sigma(T,\Omega,k)}{dTd\Omega}\frac{f(k)}{k}dk\equiv I,$$

where $m\equiv\Delta\Omega\Delta p/p$. The cross section I defined in this way will thus have the dimensions of cm^2/Mev-sr-equiv. quantum, and in Sec. IV the experimental results will be presented in the form of this quantity I. This expression simplifies considerably when the target is hydrogen because in this case T, Ω, and k are not independent. The process is a two-body one and at a fixed angle k is uniquely related to T.

B. Corrections to the Counting Rates

The remainder of this section will be devoted to a discussion of the various corrections which were applied to the measured counting rates to obtain the values of N. The corrections most carefully considered were those which affected either the π^-/π^+ ratio or the dependence of the yield on the atomic weight of the target material. Less well known is the ratio of the yields at the two angles and in fact the absolute magnitudes of the yields at either angle are subject to some systematic error also.

(1) The background counting rate was measured for each polarity of the magnet at each meson momentum studied. The highest relative background rates were observed with the lead target at the highest meson energies, namely, 25% for 310 Mev π^+ at 115° and 10% for 410 Mev π^- at 58°. The lowest was a small fraction of 1% for 110 Mev π^+ from beryllium and carbon at 58°.

(2) The thin chamber was frequently calibrated against the standard quantameter during the course of the experiment. Any error in the determination of this ratio would lead to a systematic error in the absolute values of the yields, but its effect on the π^-/π^+ ratio and on the A dependence of the yields should be negligible.

(3) A calculation of the particle orbits in the detection magnet indicated that a correction was necessary for the size of the gamma-ray beam at the experimental target location. This difficulty was reflected in the determination of the solid angles of the two telescope geometries. The values which were used resulted from both measured intercalibration ratios and magnet calculations. Several assumptions were made and it is this correction which creates the greatest uncertainty in the absolute values presented in Sec. IV, probably about $\pm 10\%$. However, this uncertainty applies only to the absolute values of the cross section and to a consideration of the angular distribution of meson production. It does not affect the A dependence of the cross sections, the π^-/π^+ ratios, or the cross-section dependence on meson energy.

(4) The thin chamber measured the photon flux which was incident on it. But the number of mesons observed was a function of some mean distribution of photons throughout the target. Accordingly, a correction was applied to the observed rates to account for this gamma-ray beam attenuation. The expression used was checked empirically. The primary relative effect of this correction falls on the beryllium because it was much shorter in radiation lengths than the other targets. The variations among the other four are quite negligible in affecting the observed A dependence.

(5) The absorption of mesons in the detection system was considered in detail. Such absorption processes (either actual or effective) occur in the bulk target and also in the air path through the magnet, in the counters themselves, and in the absorbers situated in the telescope. In the bulk target it was assumed that elastic scattering of the mesons did not represent any loss and that of all the inelastic processes only stops and the formation of stars contributed significantly to the disappearance of mesons. Throughout the remainder of the system the effect of elastic scattering was also considered.

(6) The decay in flight of mesons as they traversed the detection system resulted in an additional reduction in observed counting rates. The flight path was divided into two regions, one measured from the target to the downstream end of the magnet, the other covering just the region of the telescope. Not all of the mesons which decayed in flight were missed by the detectors because some of the μ mesons which resulted continued in the forward direction. The telescope absorbers in all cases were such that any decay μ meson which was directed into the necessary forward cone was counted, as would have been its parent π meson had the decay not occurred.

(7) The detection magnet focused mesons of a definite momentum (with an associated spread) on the counter telescope. However, mesons of the same momentum in the magnet channel necessarily had been produced at somewhat different energies in the various targets because of the different mean distances traveled in the bulk targets. The average energy lost in the targets ranged from 2 to 14 Mev and was a function of meson energy. In order to be able to compare all the yields at a particular meson energy the corrected yields for each target and angle were plotted as a function of meson energy and the final results were taken to be the extrapolated values at five different energies. Thus, although the data were measured for magnet excitations corresponding to $T=100$, 150, etc., the results will be presented at $T=110$, 160, etc., the additional 10 Mev being chosen to lie within the spread of the 2–14 Mev mean energy loss. Any error which resulted from this operation is completely negligible compared to the statistical errors of the individual points.

IV. EXPERIMENTAL RESULTS

The results will be presented in three different forms: (A) the values of the differential cross sections for positive and negative mesons separately, (B) the sum of these cross sections divided by $A^{\frac{2}{3}}$, and (C) the values

TABLE I. Cross sections for π^+ and π^- photoproduction at 58° by 1000-Mev bremsstrahlung. The quantity $I\times10^{32}$ is given and the units are cm²/Mev-sr-equiv. quantum.

Meson energy (Mev)	Target element	π^+	π^-
110	Be	52.0 ± 1.1	68.7 ± 1.4
	C	60.0 ± 1.2	55.2 ± 1.2
	Al	108 ± 3	113 ± 3
	Cu	206 ± 5	222 ± 6
	Pb	440 ±18	587 ±24
210	Be	21.5 ± 0.4	25.6 ± 0.6
	C	24.9 ± 0.5	23.8 ± 0.5
	Al	46.9 ± 1.1	47.9 ± 1.3
	Cu	86.5 ± 2.4	84.7 ± 2.4
	Pb	199 ± 8	247 ± 9
310	Be	11.6 ± 0.3	12.6 ± 0.3
	C	14.0 ± 0.3	11.7 ± 0.3
	Al	26.3 ± 0.7	23.9 ± 0.6
	Cu	50.4 ± 1.4	44.0 ± 1.3
	Pb	97.3 ± 5.7	124 ± 7
410	Be	5.50± 0.20	4.56± 0.19
	C	6.31± 0.21	3.93± 0.16
	Al	13.0 ± 0.4	8.23± 0.37
	Cu	24.7 ± 1.2	15.4 ± 1.0
	Pb	65.6 ± 5.7	42.0 ± 4.8

of the π^-/π^+ ratio. Although the data were measured using separately the two momentum channels described in Sec. II, the results have been presented as the sum of the yields from the two. The two angles at which the spectrometer was located were 57.7°±0.2° and 115.0°±0.2°.

A. Differential Cross Sections

The measured values of the quantity $I\times10^{32}$ were used to obtain the interpolated values as discussed in the previous section. These interpolated values are given in Tables I and II and the 58° results also are plotted

TABLE II. Cross sections for π^+ and π^- photoproduction at 115° by 1000-Mev bremsstrahlung. The quantity $I\times10^{32}$ is given and the units are cm²/Mev-sr-equiv. quantum.

Meson energy (Mev)	Target element	π^+	π^-
110	Be	21.9 ± 0.5	36.4 ± 0.6
	C	32.1 ± 0.8	38.6 ± 0.8
	Al	65.2 ± 1.7	67.1 ± 1.8
	Cu	116 ± 4	130 ± 4
	Pb	272 ±14	277 ±14
160	Be	6.92 ± 0.20	11.2 ± 0.3
	C	10.1 ± 0.3	11.5 ± 0.3
	Pb	95.8 ± 8.7	91.1 ±11.3
210	Be	2.98 ± 0.07	5.00 ± 0.12
	C	3.97 ± 0.09	4.60 ± 0.12
	Pb	33.0 ± 3.1	36.0 ± 3.5
310	Be	0.610± 0.029	0.82 ± 0.04
	C	0.84 ± 0.03	0.82 ± 0.03
	Pb	8.4 ± 1.8	12 ± 1
410	C		0.111± 0.019

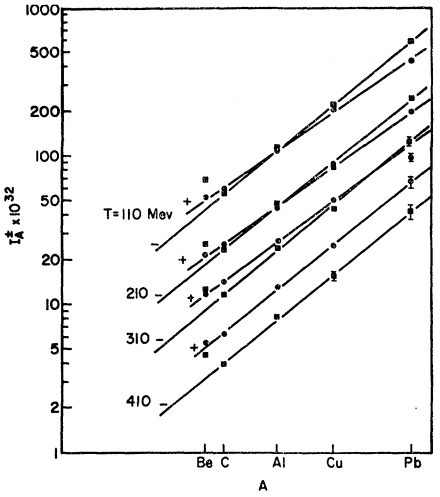

FIG. 1. π^+ and π^- cross section at 58°. The quantity I is defined in the text. The longer lines indicate the π^- data, and the high negative yield from Be is evident.

in Fig. 1. The lines there are simply a visual fit to the points.

The quantity I was defined in Sec. III to be an integrated differential cross section which can be evaluated from experimental quantities. Figure 1 demonstrates the relative production of positive and negative mesons, and also the high yield of negative mesons from beryllium is clearly in evidence here. Only statistical errors are shown.

B. A Dependence of the Cross Sections

To illustrate the observed dependence of the production on the atomic weight of target material the interpolated values of the quantity $(I^+ + I^-)/A^{\frac{2}{3}}$ were plotted using the measured values from above. These results appear plotted against A in Figs. 2 and 3 for the two angles. The lines are simply a visual fit. It is clear from these that the cross section varies with A more rapidly than $A^{\frac{2}{3}}$. The data with the single line in Fig. 3 are

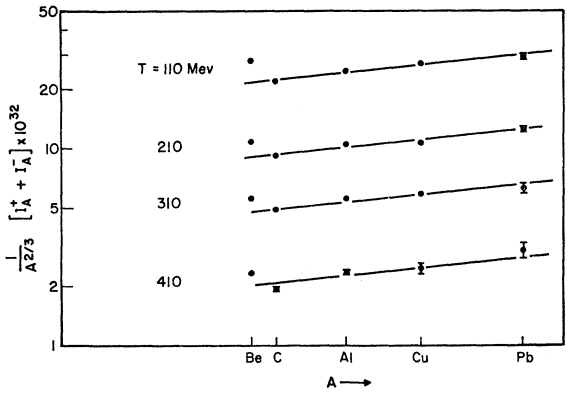

FIG. 2. A dependence of the cross section at 58°. The positive and negative data are added together and divided by $A^{\frac{2}{3}}$. The slope of the lines indicates that the dependence is steeper than $A^{\frac{2}{3}}$.

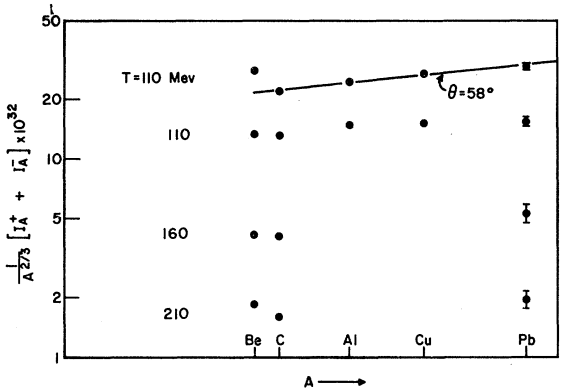

FIG. 3. A dependence of the cross section at 115°. The solid line shows the 110-Mev data from Fig. 2 for comparison. The 310-Mev results are not shown.

simply the 110-Mev data from 58° reproduced here for comparison with the 115° results. The 310-Mev data are not shown in Fig. 3.

It is of interest to characterize results such as these by their dependence on A. To this end, a linear dependence of $\log(I^+ + I^-)$ on $\log A$ has been assumed and the constant has been determined by a least-squares fit to the data of each run. However, the beryllium point has been excluded from the analysis in each case because of the high π^- contribution, which clearly deviates from the assumed dependence. The results are given in Table III.

C. π^-/π^+ Ratio

The observed π^-/π^+ ratios are shown in Table IV and plotted in Fig. 4. Because these values are plotted against meson energy it was not necessary to interpolate here. The ratios presented thus apply for each meson energy shown and any possible error from an interpolation is avoided. The horizontal line in each graph indicates the value of N/Z, the ratio of the number of neutrons to the number of protons in each nucleus. Here, as in the previous figures, only the statistical errors are shown.

TABLE III. Dependence of the sum $I^+ + I^-$ on the atomic weight of the target. Let this sum of the cross sections be proportional to A^k. Then values of k obtained by a least-squares fit to the C, Al, Cu, and Pb data are given. The Be data were not considered because of the high π^- yield.

Meson energy (Mev)	Values of k 58°	115°
110	0.77	0.72
160		0.75[b]
210	0.77	0.73[b]
310	0.75(0.79)[a]	0.87[b]
410	0.81	

[a] The (0.79) was obtained by using only C, Al, and Cu; the Pb point which appears low in Fig. 1 was thus ignored in the least-squares fit here. The 0.75 includes the Pb point.
[b] For these three entries only the C and Pb points were used (not the Be), so the values shown are not the result of a least-squares analysis.

TABLE IV. The π^-/π^+ ratio at 58° and at 115°.

Target element	Meson energy (Mev)	Ratio at 58°	Meson energy (Mev)	Ratio at 115°
Be	109	1.32 ±0.04	109	1.63 ±0.05
C	114	0.922±0.028	114	1.18 ±0.04
Al	112	1.04 ±0.04	114	1.02 ±0.04
Cu	107	1.08 ±0.04	109	1.11 ±0.05
Pb	102	1.34 ±0.08	103	1.03 ±0.07
Be			158	1.63 ±0.06
C			162	1.13 ±0.04
Pb			153	0.955±0.147
Be	208	1.20 ±0.04	207	1.67 ±0.06
C	212	0.955±0.028	212	1.15 ±0.04
Al	211	1.02 ±0.04		
Cu	206	0.984±0.039		
Pb	202	1.24 ±0.07	203	1.08 ±0.15
Be	307	1.08 ±0.04	307	1.3 ±0.1
C	312	0.841±0.028	311	0.98 ±0.05
Al	310	0.909±0.033		
Cu	306	0.884±0.036		
Pb	302	1.30 ±0.10	303	1.4 ±0.3
Be	407	0.836±0.046		
C	412	0.615±0.033		
Al	410	0.633±0.034		
Cu	406	0.640±0.053		
Pb	402	0.676±0.097		

V. INTERPRETATION OF THE RESULTS

The experimental results have been presented in the previous section. It is now of interest to determine to what extent these measurements can be understood on the basis of existing information concerning photoproduction processes. A survey of previous approaches to this problem shows that two alternatives have been proposed.

The first mechanism which was suggested assumed that the photoproduction cross section was the same for all the nucleons in a nucleus. Mesons were thus created throughout the nuclear volume and then any discussion of the observed yields of mesons necessarily dealt with the escape of these particles from the interior of the nucleus.

However, the production cross section might not be the same for all nucleons; instead the cross section could conceivably be different for nucleons in the interior of nuclei and for ones on the surface. Thus, for example, the mechanism of meson reabsorption at the point of creation could result in such an effect, and for sufficiently strong suppression of the cross section inside nuclei the photoproduction of mesons would be effectively a surface phenomenon.

In the present work only the application of the former (volume production) alternative will be investigated. It will be shown that the results are consistent with the predictions of such a model and for this reason no recourse to the surface production model will be necessary.

The complications brought about by the use of heavier nuclei as targets necessitate the development of

a model in which the basic cross sections can be incorporated together with some consideration of the pertinent nuclear features. The cross sections for the photoproduction of mesons on hydrogen and on deuterium are useful in such a program and the model to be employed here will utilize this information to determine the initial production of mesons throughout the nuclear volume. The escape of the mesons will then be treated by considering nuclear matter as an optical medium characterized by an absorption coefficient and an index of refraction.[17] The results of meson-nuclear scattering experiments can be analyzed by assuming the existence of a complex potential within a nucleus.[18] In analogy to optics, the complex index of refraction can then be expressed in terms of V_R, V_I, and the energy of the meson, and an interaction mean free path is in turn related to the imaginary part of this index of refraction.[10] In the present work V_R will be taken to be the change in

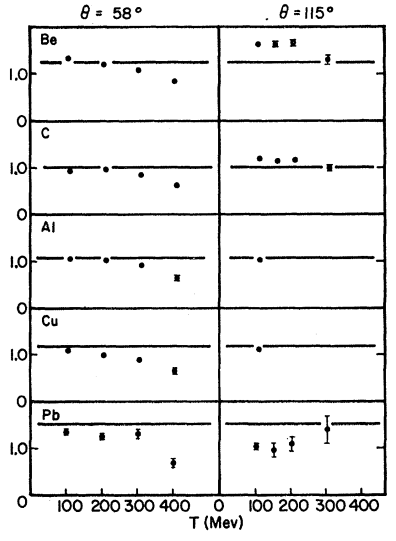

FIG. 4. π^-/π^+ ratio at 58° and at 115° as a function of meson energy. The data for five elements are shown. The solid line in each case indicates the value of N/Z.

energy experienced by a meson as it leaves the nucleus and the mean free path will be used to calculate the expected transmission of mesons through nuclear matter. Both reflection and refraction at the nuclear surface will be ignored. This should not cause much difficulty. The effects of refraction should be small compared to the angular variations resulting from the initial photoproduction process and the subsequent inelastic scatterings. Reflection at the nuclear surface should become negligible for sufficiently high meson energies. In the case of the lowest energy studied the energy inside the nucleus is 150 Mev with a well depth of 40 Mev and this situation would exhibit reflection

[17] S. Fernbach, R. Serber, and T. B. Taylor, Phys. Rev. **75**, 1352 (1949).

[18] R. M. Frank, J. L. Gammel, and K. M. Watson, Phys. Rev. **101**, 891 (1956).

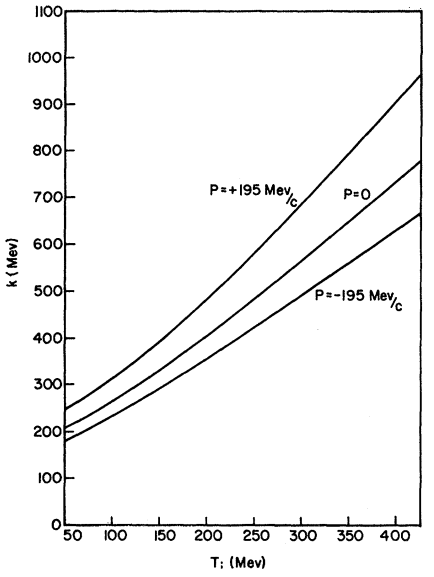

FIG. 5. Kinematics at 58°. P is the momentum of the target nucleon.

properties small enough to be ignored in the model which will be used.

A. Development of the Model

It is instructive to begin with a consideration of the kinematics involved at the two angles. The middle curve in Fig. 5 shows the photon energy required to produce from a stationary target nucleon a meson of kinetic energy T_i at 58° in the laboratory system. Figure 6 shows the same information for a laboratory angle of 115°. These would be the pertinent kinematic curves

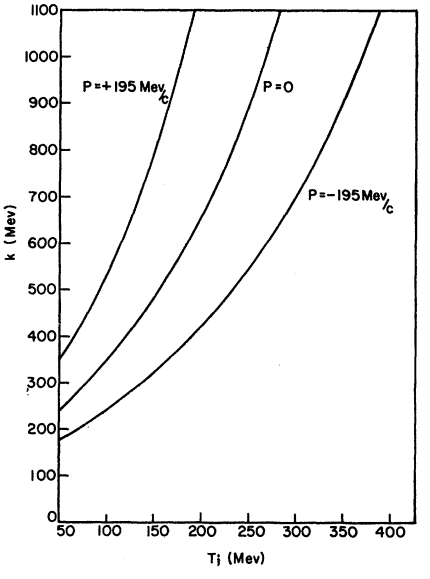

FIG. 6. Kinematics at 115°. P is the momentum of the target nucleon.

for a target of hydrogen. But for any heavier nuclear target, the nucleons are not likely to be stationary, but in fact can have their motion characterized by some particular momentum distribution. The other curves in the two figures are intended to demonstrate the effect of such target motion on the kinematics. The top curve in each figure applies to the case of a target nucleon which moves in the same direction as the incident photon with a momentum of 195 Mev/c (kinetic energy of 20 Mev), while the bottom curve applies to a nucleon of the same energy which moves toward the photon. It should be emphasized that these curves refer to free nucleons, either moving or stationary, and as such are not directly related to the case of moving nucleons in a nucleus. In the latter instance the presence of nuclear potentials has the effect of lowering the necessary photon energy somewhat.[13]

For the present experiment with a peak photon energy of 1000 Mev, Fig. 6 indicates that it would be impossible to produce, for example, a 300-Mev meson at 115° from a hydrogen target; this would require a 1250-Mev photon. But the internal momentum distribution of the nucleons in a nucleus relaxes this condition to the extent that some of the nucleons can serve as targets for such a process. This assumes that the photon interacts with a single nucleon in the nucleus and this assumption will be used throughout the analysis.

The higher energy data at 115° were measured specifically for the purpose of investigating this nuclear effect on the kinematics. According to the discussion above, the number of target nucleons will not necessarily be Z or N, but in fact will depend on the photon energy available, the meson energy and direction, and the momentum distribution of the nucleons. Brueckner, Serber, and Watson[9] approximated the cross section for positive meson photoproduction by the expression

$$\sigma_A = Z\eta\sigma_P f_a,$$

where Z is the number of target protons, σ_P is the photoproduction cross section for a free proton, and η represents the effects of nuclear binding. The factor f_a represents the fraction of mesons produced in the nucleus which are not absorbed before escaping.

The model to be used here represents several modifications of this expression, but the basic idea remains the same. The similarities and variations will be listed here.

(1) The model applies only to the photoproduction of single mesons. The effect of meson pairs will be discussed later. Thus the Z protons will act as targets for π^+ production and the N neutrons for π^-.

(2) However, the momentum distribution of these target nucleons can render some of them ineffective in any particular process. Thus this distribution function must have an effect on the measured yields.

(3) As in the model of Brueckner *et al.*, the free proton cross section will be used in the expression for the π^+ nuclear cross section. The hydrogen data of Turkot[19] at laboratory angles of 58° and 115° can be used directly here. No such free neutron cross sections exist; instead it will be assumed that the neutron cross section for the photoproduction of π^- mesons will be given by the product of the appropriate free proton cross section and the π^-/π^+ ratio for deuterium. This ratio has been measured by Neugebauer, Wales, and Walker[20] and values interpolated from their data will be used.

(4) Because of the existence of a meson-nucleus interaction the kinetic energy of the meson at creation inside the nucleus T_i is different from its detected kinetic energy T outside the nucleus. This interaction consists of two parts; the Coulomb potential depends on the atomic weight of the target nucleus, while the π-nuclear potential does not. In general the (non-Coulomb) interaction between a meson and a nucleus can be characterized by a complex potential, the real part of which describes the elastic scattering of the meson, and the imaginary part characterizes the inelastic processes. Values of V_R can be determined from the results of π-nucleus scattering experiments, and Frank, Gammel, and Watson[18] have calculated V_R from pion-nucleon scattering cross sections. Several experimental determinations appear in the literature.[21–23] With this total π-nucleus potential the kinetic energy of a meson inside a nucleus can be related to its energy outside. The change in kinetic energy experienced by a meson in escaping from a nucleus thus depends on the charge of the meson, the atomic number of the nucleus, and the energy of the meson.

(5) The recoil nucleon similarly experiences a change in kinetic energy upon leaving the nucleus, and this change (except for Coulomb effects) is given by the real part of the nucleon-nucleus optical model potential. Values of this nucleon potential, derived from the results of various scattering experiments, are given by Riesenfeld and Watson.[24] There appears to be some difference in this potential for neutrons and protons below 50 Mev.[25] The energy change of the nucleon thus depends on the charge of the meson being produced, the atomic number of the target nucleus, and the energy of the recoil nucleon.

In Sec. III the cross section for the photoproduction of charged mesons from nuclei was related to the measurable quantities of this experiment. To express this nuclear cross section in terms of the known free-

[19] F. Turkot, Ph.D. thesis, Cornell University, 1959 (unpublished).
[20] G. Neugebauer, W. Wales, and R. L. Walker, Phys. Rev. **119**, 1726 (1960).
[21] T. A. Fujii, Phys. Rev. **113**, 695 (1959).
[22] E. C. Fowler, W. B. Fowler, R. P. Shutt, A. M. Thorndike, and W. L. Whittemore, Phys. Rev. **91**, 135 (1953).
[23] K.-C. Wang, T.-T. Wang, D. T. Ding, L. N. Dubrovskii, E. N. Kladnitskaia, and M. I. Solov'ev, Soviet Phys.—JETP **8**, 625 (1959); M. S. Kozodaev, R. M. Sulaev, A. I. Filippov, and I. A. Shcherbakov, Soviet Phys.—JETP **4**, 580 (1957).
[24] W. B. Riesenfeld and K. M. Watson, Phys. Rev. **102**, 1157 (1956).
[25] A. M. Lane, Revs. Modern Phys. **29**, 191 (1957).

nucleon cross sections is the goal of the present section. In spite of the many approximations employed the over-all result of this attempt seems to lend further support to the twofold scheme of treating the nucleons as separate targets and then of using the notion of the optical model to characterize the subsequent interactions of the mesons in nuclear matter.

Following the prescription outlined above, the total number of mesons produced in nuclei can be approximated by an expression involving integrations over both the bremsstrahlung spectrum and the momentum distribution of the nucleons. In the case of hydrogen, the nucleon momentum is taken to be zero and a photon of specific energy is defined by the energy and direction of the produced meson. For heavier targets the nucleons are moving and in fact it is possible to choose the meson energy and direction to represent so stringent a condition that the nucleons can serve as targets only by virtue of their motion. In general, a range of photon energies will contribute to the nuclear production of mesons, subject at one extreme to the maximum energy of the bremsstrahlung beam and at the other to the details of the threshold for the process. For this model, in which individual nucleons are considered, the energy and momentum of the photon-struck nucleon system are taken to be conserved. These conservation conditions relate the photon energy, the target nucleon motion, and the resulting meson energy and direction. The nucleon momentum distribution is generally taken to be Gaussian[26] and this permits the evaluation of the integral over the nucleon momenta. The result is expressed finally as one integral over the photon energy and this can be evaluated numerically for each case of interest. Starting from the expression for the number of mesons produced inside nuclei, the quantity $N/nQmp(dT/dp)$ can be formed and this will be designated by the symbol I' to be distinguished from the experimental quantity of Sec. IV. N refers to the number of mesons actually detected and therefore the expression for I' contains a factor f which represents the fraction of produced mesons which manage to escape from the parent nuclei.

B. Energy Dependence of the Cross Section

Because the extent of the nuclear effects on the kinematics depends on the meson energy, it is interesting to investigate the predictions of the model in this respect first. I' was calculated for various meson energies at the two angles. Wattenberg *et al.*[26] give the following results from their experiment for E_g: Li, 9.0±1.0 Mev; C, 19.7±1.5 Mev; and O, 19.7±2.5 Mev. Most of the calculations were done for carbon with the choice, $E_g=20$ Mev; a few values were obtained for lead using the same value for E_g. The numbers I'/f thus give the predicted production of mesons inside the nuclei, whereas the I' to be determined are expected to give the actual measured yields.

It remains to calculate the appropriate values of f, the transmission factor for mesons in nuclear matter. The fact relies on the concept of a mean free path based on the optical model. In general for a nucleus of radius R and a particle of mean free path λ, the probability $P(n)$ that a particle, produced at random inside a nucleus, makes exactly n collisions before escaping can be calculated. For the present application only $P(0)$ is required. This is the probability that the particle escapes without experiencing any collision. This is the quantity f_a mentioned above. It is given by the equation

$$P(0)=\frac{1}{V_A}\int e^{-D/\lambda_a}d\tau=3\left[\frac{1}{2x}-\frac{1}{x^3}+\frac{(1+x)}{x^3}e^{-x}\right],$$

where the integration is taken over the nuclear volume, D is the distance the meson travels before escaping, and x is defined by the relation $x\equiv 2R/\lambda_a$, where R is the nuclear radius. Here λ_a is the mean free path for the absorption of mesons, and thus f_a gives the probability that a meson escapes without being absorbed.

However, this factor f is calculated on geometrical grounds and depends only on R and λ; thus any λ may be used with a corresponding interpretation of f. In particular for the present analysis the total mean free path will also be used. This is defined by the relation[9,18]

$$1/\lambda_t=1/\lambda_s+1/\lambda_a,$$

where λ_t is the mean free path for either an inelastic scattering or an absorption of the pion by the nucleus. λ_s is the mean free path for an inelastic process.

λ_s and λ_a can be related to π-nucleon scattering cross sections if it is assumed that the mesons interact in the nucleus with the individual nucleons. Ignatenko[27] gives evidence that this is the case for mesons in the range 30–350 Mev; above 140 Mev, it is claimed that Pauli principle effects can probably be neglected safely. The determination of λ_a has been discussed by several authors.[10,18,28] Meson absorption is assumed to occur in a two-nucleon process in which one nucleon absorbs the meson and then scatters from a second nucleon. Because of the conservation of charge, the absorbing nucleon must be a neutron for π^+ absorption and a proton for π^- absorption.

Thus a knowledge of these various cross sections permits the determination of both λ_a and λ_t. Each may be used in the quantity $2R/\lambda$ and the resulting f_a and f_t will have appropriate meanings. f_a gives the fraction of produced mesons which are not absorbed before escaping from the nucleus; f_t similarly gives the fraction

[26] A. Wattenberg, A. C. Odian, P. C. Stein, H. Wilson, and R. Weinstein, Phys. Rev. **104**, 1710 (1956).

[27] A. E. Ignatenko, *Proceedings of the CERN Symposium on High-Energy Accelerators and Pion Physics, Geneva, 1956* (European Organization of Nuclear Research, Geneva, 1956) Vol. II, p. 313.

[28] N. Metropolis, R. Bivins, M. Storm, J. M. Miller, G. Friedlander, and A. Turkevich, Phys. Rev. **110**, 204 (1958).

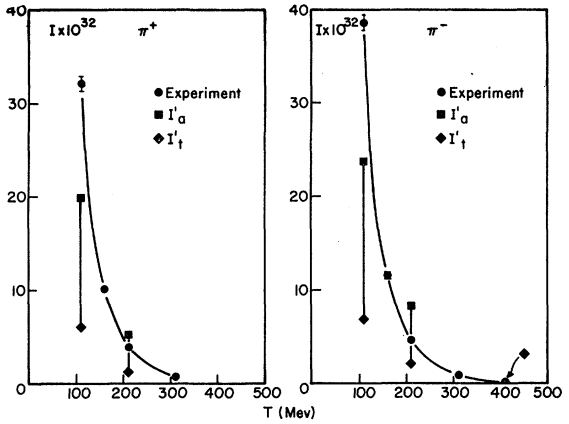

FIG. 7. Measured and computed results for carbon at 115°. The π^+ and π^- data are shown separately. The solid curve connects the experimental points. The vertical lines indicate the range predicted by the model, but at 410 Mev only one such value is given.

of mesons which do not interact at all (a scattering or an absorption) before escaping.

It is assumed that a number of mesons are produced in the nucleus and that these then make their way to the surface. Each meson has a "choice" whether to interact or not. The factor f_t gives the fraction which does not interact at all, i.e., the probability that a meson makes zero collisions in escaping. Certainly these mesons should be detected, as they experience no difficulty in leaving the nucleus. Because many of the mesons which do interact will also escape, application of f_t in the expresion for I' should give a lower limit to the experimental results.

Furthermore, if the fraction f_t of the initially created mesons experience no interaction, then the remaining fraction $(1-f_t)$ of them do interact. This may be either an absorption or a scattering. If a gives the fraction of interactions which results in an absorption, then $(1-f_t)(1-a)$ of the initial number of mesons scatter and are available to make a second "choice." Again there are three alternatives, namely, escape with no further interaction, absorption, or scattering with the option of making a third "choice." The extent to which this process repeats is governed by the size of the nucleus compared to the length of the particular total mean free path being considered.

Each time a "choice" is made, some mesons are absorbed. f_a will give the fraction which are not absorbed, so $(1-f_a)$ must be the fraction which do experience absorption and this latter quantity must be just the sum of all the separate contributions resulting from the succession of "choices." In order to calculate f_a it is assumed that the mean free path of interest is λ_a, not λ_t, and thus inelastic scatterings are ignored; although a meson changes energy and direction in such a process, it does not disappear. It is then expected that $(1-f_a)$ of the initial meson number cannot be detected and, just as f_t should set a lower limit on the predicted yields, f_a should set an upper one.

TABLE V. Comparison of the computed and measured cross sections. The quantities I_t' and I_a' are the computed cross-section limits discussed in the text (in cm²/Mev-sr-equiv. quantum). The last column shows the measured results for comparison.

Element	Angle	Meson energy (Mev)	Charge	$I_t'\times10^{32}$	$I_a'\times10^{32}$	$I\times10^{32}$
C	115°	110	+	6.04	19.9	32.1 ±0.8
		110	−	6.89	23.7	38.6 ±0.8
		210	+	1.30	5.20	3.97 ±0.09
		210	−	2.09	8.29	4.60 ±0.12
		410	−	0.199	0.344	0.111 ±0.019
Pb	115°	210	+	7.14	39.6	33.0 ±3.1
		210	−	16.6	130	36.0 ±3.5
C	58°	210	+	4.24	17.0	24.9 ±0.5
		210	−	4.87	19.3	23.8 ±0.5
		410	+	7.28	12.8	6.31 ±0.21
		410	−	6.06	10.5	3.93 ±0.16

It thus remains to calculate the values of f_t and f_a for the various cases. Charge symmetry may be assumed and then the experimental scattering cross sections serve to determine the mean free paths. The final results are given in Table V, where for each computed value of I' two entries appear, one using f_t and labeled with a subscript t, the other using f_a with a corresponding subscript. In the last column the appropriate measured results of Sec. IV are shown for comparison. Finally Figs. 7, 8, and 9 show complete sets of data for carbon and lead together with the computed I_t' and I_a' values for the cases considered. The curve in each figure goes through the experimental data, and the vertical lines extend from I_t' to I_a'.

Several comments can be made in general before the particular cases are considered individually.

(1) In the model used here the hydrogen cross sections measured at 58° and 115° were used directly and nowhere in the model has any attempt been made to account for any angular dependence effects due to the inelastic processes. The model assumed the creation of a flux of mesons leaving the nucleus at either 58° or 115° to the photon beam and it was to this idealized flux that the transmission factor was applied.

(2) The detailed effects of the inelastic processes have not been considered. The possibility of π production by the mesons as they scatter from nucleons is slight, but charge exchange scattering should be common. Metropolis *et al.*[28] give the probabilities for the various inelastic processes as functions of the meson energy. In each inelastic encounter the meson loses energy and this degradation has the effect of removing particles from the energy channel in which they were produced. Thus, for all but the highest energy data, it is likely that some of the mesons detected actually had higher energy at creation. It is for this reason that the f_t and f_a were used in the analysis. The fraction f_t did not interact and hence they should be detected at the T corresponding to the T_i they had at production. In contrast those of the remaining $(1-f_t)$ which were not absorbed can emerge with any energy below T.

(3) The experimental data are given as absolute measurements and as such are subject to the systematic uncertainties associated with the experimental technique. In like manner absolute predictions of the cross sections were obtained from the model. The extent of the agreement between the predictions and the data thus rests directly, for example, on the choice of E_g used in the model. As a value for E_g was found only for carbon, the application of the model to other elements suffers from this uncertainty.

(4) The situation in the vicinity of threshold was treated by a rough approximation which resulted in a low-energy cutoff in the integration over the bremsstrahlung spectrum. For successively lower meson energies such a procedure introduces relatively larger uncertainties in the results. A similar increase in uncertainty with decreasing meson energy results from the degradation effects of inelastic processes. Mesons detected at 110 Mev are likely to have a greater variety in their histories than ones at 410 Mev.

With this preface the individual cases can now be discussed briefly.

1. Carbon at 115°

410 Mev. Here production from hydrogen would be impossible, so the extent of the agreement is interesting. At this energy absorption of the mesons is unlikely; however, any inelastic event would have the effect of removing the meson from that energy channel inside the nucleus which results in 410 Mev outside. In fact, the measured value is even below I_t'. No attempt will be made to explain the discrepancy because at least four effects could combine to render such an attempt futile. First, the choice for the value of E_g and the systematic uncertainty in the data would have to be re-examined. Second, because such mesons were produced by the highest energy photons available, the exact way in which the photon beam was spread in energy would possibly affect the data, but this was ignored in the model. Third, the results from the two counter channels in the telescope were combined, but at this high meson energy the centers of the channels were more than 50 Mev apart and the data must represent some average yield over this broad interval of meson energy, while the computed yield was calculated at 410 Mev. Finally the uncertainty in the threshold location, although not severe here, might have an effect.

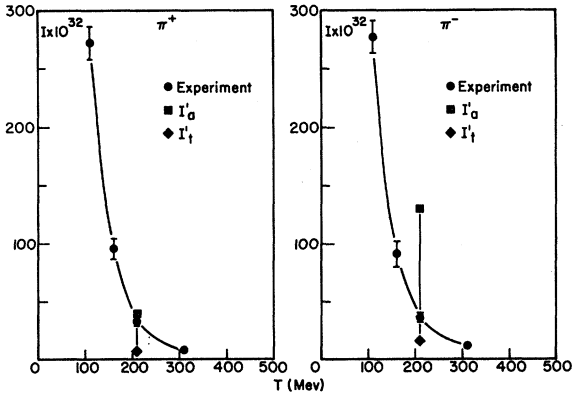

FIG. 8. Measured and computed results for lead at 115°.

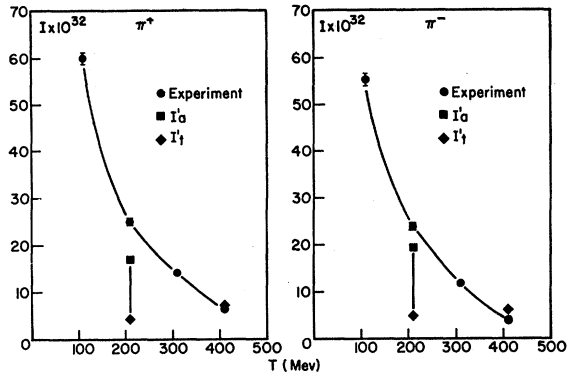

FIG. 9. Measured and computed results for carbon at 58°. Only one value is predicted by the model at 410 Mev.

210 Mev. Here the measurements lie within the predicted range. The gain and loss resulting from inelastic processes are likely to cancel partially and the threshold effect should not be too significant here.

110 Mev. The predictions fall short of the measurements for at least two reasons. Degradation due to inelastic processes would be expected to enhance the number of detected lower-energy mesons. Also the threshold location now becomes important and it is possible that the cutoff, being in a sensitive region, resulted in something less than the full value of the integral. Both effects would improve the agreement between the measured and predicted values.

2. Lead at 115°

210 Mev. The value of E_g for carbon was used for this one case with lead. This particular choice was made because of the good agreement in the carbon data at this energy and angle.

3. Carbon at 58°

410 Mev. As for 410 Mev at 115°, I_t' is the more reasonable prediction here. At 410 Mev absorption is negligible so $f_a=1$, and thus I_a' is just the total number of mesons initially created.

210 Mev. This case is similar to the 110-Mev, 115° situation. However, in addition to the effects discussed there, it is important to realize that around 200 Mev, the total mean free path is at a minimum and, because of the likelihood of multiple collisions, the data must represent the effects of considerable mixing both in angle and in energy.

110 Mev. No prediction was made here for two reasons. First, the threshold effect, already likely to be important

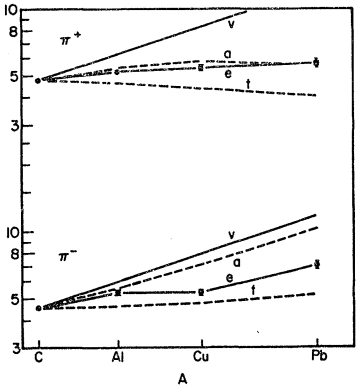

FIG. 10. Measured and computed A dependence for 210-Mev mesons at 58°. The general quantity $(I/A^{\frac{2}{3}})\times 10^{32}$ is plotted vertically for π^+ and π^-. The solid lines labeled v indicate the behavior of a cross section linear in A, while a horizontal line (not shown) would apply to a cross section proportional to $A^{\frac{2}{3}}$. The dashed lines labeled a and t define the limits given by the model, and the experimental points are shown with their statistical errors. The a and t curves suggest a steeper dependence on A for the π^- at this energy, and this behavior is shown clearly in Fig. 1. All curves are normalized at carbon.

at 210 Mev, would cause an even greater uncertainty here. However, even more important is the contribution to the measured meson yields from meson pair photoproduction. Bloch and Sands[29] give the negative meson yield from hydrogen at 60° as a function of bremsstrahlung cutoff energy for several meson energies. In particular the yield for a meson energy of 148 Mev at 60° for $k_0=1000$ Mev is given to be 1.1×10^{-32} cm²/Mev-sr-equiv. quantum. Taking $T_i=148$, these conditions are ideal for comparison with the $T=110$ data at 58° of the present experiment. For example, with a carbon target the six protons would be expected to contribute 6.6×10^{-32} to I'/f, the initial number of negative mesons. These are in addition to those produced in both single and pair production on the neutrons. The measured result of the present experiment for 110 Mev negative mesons from carbon at 58° is $55.2\pm 1.2\times 10^{-32}$, so it is clear that the effect of pair photoproduction is not negligible. A similar situation exists for positive mesons. The meson pair data indicate that the effect of pairs is likely to be significant only for the 110-Mev, 58° data of the present experiment.

C. Ratio of the π^- to π^+ Cross Sections

The measured ratios presented in Table IV and in Fig. 4 exhibit the same general behavior as the π^-/π^+ ratios for deuterium,[20] with the exception of the lead data at 115°. The similarity is particularly striking at 58°, where the observed ratios drop appreciably below N/Z values in the same way that the deuterium data drop below unity. The changing numbers of effective proton and neutron targets at 115° would make detailed analysis of the ratios at that angle especially difficult.

However, because the model does not give unique predictions for the cross sections, no definite ratios are obtained either. The model was not intended to predict ratios; the π^-/π^+ ratio depends too sensitively on many features of the actual process which have been neglected.

D. Dependence of the Cross Section on the Atomic Weight of the Target

The last particular feature of the data to be considered is the A dependence of the cross sections. It was mentioned in the Introduction that a dependence on the atomic weight of $A^{\frac{2}{3}}$ was the common result obtained by workers using bremsstrahlung beams of peak energies up to 550 Mev. The highest meson energy reported was 152 Mev in reference 4.

However, Waters[5] and the present experiment have measured meson yields from bremsstrahlung beams of 1000-Mev peak energy, the former for mesons of energies 40 and 80 Mev, the latter for 110 to 410 Mev. The present experiment finds evidence for an $A^{\frac{2}{3}}$ dependence, so it is interesting to examine the results of Waters. In particular the production of 80-Mev π^+ mesons was measured by him for both an 800-Mev bremsstrahlung beam and a 1000-Mev one at a laboratory angle of 35°.

A least-squares fit to the C, Al, Cu, and Pb data (the same elements discussed in Table III) yields an A dependence of $A^{0.72}$ for both the $k_0=800$-Mev and the $k_0=1000$-Mev data. Waters tried to improve upon the optical model results by considering the effect of an inelastic scattering process. In this way he succeeded in obtaining somewhat better agreement between his results and the calculated A dependence, but the latter still did not vary rapidly enough with A to fit the data.

The model used in the present analysis cannot be applied to such an investigation, however, unless E_g is known for each element. But a knowledge of E_g should be necessary only when the effect of the nucleon momentum distribution is important. In the case of 210-Mev data at 58°, for example, it seems clear that all of the nucleons can contribute, and so an integration over the momentum distribution would give unity, independent of E_g. This scheme should be acceptable whenever all of the nucleons can act as targets and when details of the kinematics are not important.

Using this idea, an expression can be derived from the original model which should be suitable for calculating the relative A dependence. As this now is an attempt to investigate only the A dependence of the cross sections, the calculated and measured values of $I/A^{\frac{2}{3}}$ will be normalized at carbon. Values of f_t and f_a can be calculated for aluminum and copper just as these quantities were determined for carbon and lead. The results of the calculation and the experimental data for 210 Mev, 58° are plotted in Fig. 10.

[29] M. Bloch and M. Sands, Phys. Rev. **113**, 305 (1959).

A horizontal line in this figure would correspond to an $A^{\frac{2}{3}}$ dependence and the solid lines shown there indicate a dependence linear in A. It is apparent that the experimental points do lie between the limits defined by f_t and f_a. Furthermore the difference in A dependence for the π^+ and π^- cross sections, which is demonstrated in Fig. 1, is clearly predicted by the modified model employed here. Thus, although the particular A dependence of the data has not been calculated, the origin of the essential features has been shown.

ACKNOWLEDGMENTS

The author is indebted to Professor W. M. Woodward for suggesting the problem and for his help during the course of the experiment. He would like to thank Professor B. D. McDaniel for several constructive suggestions in the early phase of the work. Also, he would like to express his appreciation to the entire synchrotron staff whose combined efforts made this investigation possible.

PHYSICAL REVIEW VOLUME 123, NUMBER 4 AUGUST 15, 1961

Secondary Cosmic-Ray Photons below Cascade Energy*

KINSEY A. ANDERSON
Department of Physics, University of California, Berkeley, California
(Received April 7, 1961)

Investigations with small unshielded scintillation crystals carried through the atmosphere by balloons, show large fluxes of photons in the energy region 30 to 300 kev in equilibrium with the primary cosmic ray beam. At 90 g cm^{-2} depth the flux is about 22 photons cm^{-2} sec^{-1} compared with a charged particle flux determined from a Geiger tube of 1.9 cm^{-2} sec^{-1} at this same depth. The photon flux at zero depth, taken to be the albedo of this secondary cosmic-ray component, has been estimated by extrapolation to be 8 photons cm^{-2} sec^{-1} greater than 30 kev.

INTRODUCTION AND DESCRIPTION OF APPARATUS

ON a number of occasions during 1958 and 1959 scintillation spectrometers have been included in balloon borne payloads designed to study cosmic rays and auroral zone x-ray effects. Results from flights in the auroral zone, where frequent but sporadic influxes of x rays are occurring, have been published previously.[1,2] The purpose of the present discussion is to present some results concerning photons in the energy region 30 to 300 kev in equilibrium with the primary cosmic-ray beam and therefore always present in the atmosphere.

The experimental apparatus pertinent to the discussion is described in Table I. Scintillation counter data from only one balloon flight will be presented here, but several other flights have also led to the same results within experimental uncertainties involved in determining the atmospheric depth, the setting and stability of the discriminator edges, and the statistical fluctuations in the counting rates.

RESULTS

Figure 1 shows the ratio of the Geiger-Müller tube, counting rate to its geometry factor as a function of atmospheric depth. The detection efficiency of this tube for photons is less than $\frac{1}{2}\%$ at all energies, so that the ordinate of this plot represents very nearly the charged particle flux inside the cosmic-ray gondola assuming this flux to be isotropic over the upper hemisphere.

Figure 2 shows the counting rates in the four integral channels of the pulse-height analyzer divided by the geometry factor of the sodium iodide crystal determined from the same formula as the Geiger-Müller tube. The counting rate to geometry-factor ratio in the 34-kev channel of the scintillation counter is seen to be very much greater than that for the Geiger-Müller tube despite the fact that the crystal has a slightly thicker shielding. The crystal has an efficiency between 1 and 0.5 for detecting photons in the energy region 30 to 300 kev and unit efficiency for detecting charged particles entering its active region. From this it is concluded that the flux of photons must be much higher than the flux of charged particles at all depths in the atmosphere. This result is emphasized by Fig. 3.

To obtain the flux of photons present in the atmosphere (using the hemispherical geometry factor), two corrections have been applied to the scintillation counter data of Fig. 2. First, the charged particle flux as measured by the Geiger-Müller tube has been subtracted from all channels of the scintillation counter. This may be a slight overcorrection since the Geiger tube has a somewhat smaller wall thickness than the crystal. The analysis here uses results from a Geiger-Müller tube flown on a different day from the scintillation counter measurements. The Geiger-Müller tube was flown on August 4, while the scintillation counter measurements were taken on August 8, 1959. The Deep River neutron

* This work supported by the Office of Naval Research. It was a part of the U. S. participation in IGC 1959.
[1] K. A. Anderson, J. Geophys. Research **65**, 551 (1960).
[2] K. A. Anderson and D. C. Enemark, J. Geophys. Research **65**, 3521 (1960).